blood®
Regular Article

Check for updates

TRANSPLANTATION

Signatures of GVHD and relapse after posttransplant cyclophosphamide revealed by immune profiling and machine learning

Shannon R. McCurdy,[1,*] Vedran Radojcic,[2,3,*,†] Hua-Ling Tsai,[4] Ante Vulic,[5] Elizabeth Thompson,[5] Sanja Ivcevic,[2,3] Christopher G. Kanakry,[6] Jonathan D. Powell,[4] Brian Lohman,[3] Djamilatou Adom,[6] Sophie Paczesny,[7,8] Kenneth R. Cooke,[4] Richard J. Jones,[4] Ravi Varadhan,[5] Heather J. Symons,[4] and Leo Luznik[4,†]

[1]Abramson Cancer Center and the Division of Hematology and Oncology, Hospital of the University of Pennsylvania, Philadelphia, PA; [2]Division of Hematology and Hematologic Malignancies, Department of Internal Medicine, University of Utah, Salt Lake City, UT; [3]Huntsman Cancer Institute, University of Utah, Salt Lake City, UT; [4]Department of Oncology and the Sidney Kimmel Comprehensive Cancer Center, The Johns Hopkins University School of Medicine, Baltimore, MD; [5]Division of Biostatistics and Bioinformatics and the Sidney Kimmel Comprehensive Cancer Center and The Johns Hopkins University School of Medicine, Baltimore, MD; [6]Experimental Transplantation and Immunology Branch, Center for Cancer Research, National Cancer Institute, National Institutes of Health, Bethesda, MD; [7]Department of Pediatrics, Indiana University School of Medicine, Indianapolis, IN; and [8]Department of Microbiology and Immunology and Pediatrics, Medical University of South Carolina, Charleston, SC

KEY POINTS

- **Conventional CD4$^+$ T cell recovery, their activation status, and metabolic signatures are risk markers for aGVHD.**
- **Early NK cell recovery protects against relapse, while loss of NK and CD8$^+$ T cell inflammatory signaling predominates in relapsing patients.**

The key immunologic signatures associated with clinical outcomes after posttransplant cyclophosphamide (PTCy)-based HLA-haploidentical (haplo) and HLA-matched bone marrow transplantation (BMT) are largely unknown. To address this gap in knowledge, we used machine learning to decipher clinically relevant signatures from immunophenotypic, proteomic, and clinical data and then examined transcriptome changes in the lymphocyte subsets that predicted major posttransplant outcomes. Kinetics of immune subset reconstitution after day 28 were similar for 70 patients undergoing haplo and 75 patients undergoing HLA-matched BMT. Machine learning based on 35 candidate factors (10 clinical, 18 cellular, and 7 proteomic) revealed that combined elevations in effector CD4$^+$ conventional T cells (Tconv) and CXCL9 at day 28 predicted acute graft-versus-host disease (aGVHD). Furthermore, higher NK cell counts predicted improved overall survival (OS) due to a reduction in both nonrelapse mortality and relapse. Transcriptional and flow-cytometric analyses of recovering lymphocytes in patients with aGVHD identified preserved hallmarks of functional CD4$^+$ regulatory T cells (Tregs) while highlighting a Tconv-driven inflammatory and metabolic axis distinct from that seen with conventional GVHD prophylaxis. Patients developing early relapse displayed a loss of inflammatory gene signatures in NK cells and a transcriptional exhaustion phenotype in CD8$^+$ T cells. Using a multimodality approach, we highlight the utility of systems biology in BMT biomarker discovery and offer a novel understanding of how PTCy influences alloimmune responses. Our work charts future directions for novel therapeutic interventions after these increasingly used GVHD prophylaxis platforms. Specimens collected on NCT0079656226 and NCT0080927627 https://clinicaltrials.gov/.

Introduction

Delayed immune reconstitution is associated with enhanced infectious and relapse risk after allogeneic blood or marrow transplantation (alloBMT)[1-3] and was an early barrier to successful alternative donor transplantation.[4-7] Posttransplantation cyclophosphamide (PTCy) enabled HLA-haploidentical (haplo) alloBMT by limiting excess nonrelapse mortality (NRM) and has been increasingly used in the HLA-matched setting.[8-13] Mechanisms responsible for the reduction in acute and chronic graft-versus-host disease (aGVHD and cGVHD) after PTCy and characterization of the unique immune milieu evident in the different patterns of GVHD remain poorly understood.[14]

PTCy has been postulated to act as an alloreactive T cell-depleting agent. However, recent studies have revealed relative sparing of alloreactive T-regulatory cells (Tregs) and association with hyporesponsive effector T cell phenotypes, suggesting GVHD-prevention mechanisms distinct from that of conventional prophylaxis.[15-19] Furthermore, data showing that PTCy may promote NK cell depletion followed by recovery to a functionally immature state underscores the importance of understanding not only the kinetics of immune recovery, but also markers of functionality and their influence on clinical outcomes.[20,21] Our previous work in PTCy-treated patients showed a correlation between day 30 levels of STimulation-2 (ST-2), CD25, tumor

Downloaded from http://ashpublications.net/blood/article-pdf/139/4/608/1864234/bloodbld2021013054.pdf by guest on 07 May 2024

© 2022 by The American Society of Hematology

necrosis factor receptor 1 (TNFR1), and regenerating islet-derived 3-α with NRM and CD25 with aGVHD development.[22] However, the biologic underpinnings of these findings, along with the interactions among proteomic, immunologic, and transcriptional signatures and their impact on survival after PTCy-based allografting have not been defined.

One of the difficulties in addressing complex posttransplant interactions is the abundance of contributing factors and the many time points at which they can be examined. Machine learning employs data-driven statistical modeling approaches that integrate multiple variables in a predictive model to identify underlying patterns and cut-points without predefined assumptions. This approach eliminates the effect of selection bias in choosing and categorizing variables and identifies associations that may not emerge in univariate analyses. Machine learning tools have been used to profile the association of immunological variables with clinical outcomes in several disease states.[23-25] Here, we use them to identify the link between biologic variables and clinical outcomes, guide correlative and preclinical studies, and generate data supporting future translational interventions.

Methods

This unplanned analysis was performed on prospectively collected samples on 75 patients who received PTCy-based alloBMT using an HLA-matched sibling (MSD) or unrelated (MUD) donor (NCT00809276[26]) and 70 patients who received haplo alloBMT (NCT00796562[27]). All patients were treated with myeloablative conditioning and received T cell replete bone marrow (BM) grafts. Clinical data reflect the patient population as a whole with detailed clinical outcomes previously published.[26,27] A total of 17/92 patients were excluded from the HLA-matched clinical trials and 26/96 patients from the HLA-haploidentical clinical trials due to graft failure, early death, or too few samples.

Classification and regression tree (CART)[28] machine-based learning was applied for overall survival (OS) treated as a time-to-event outcome, and for aGVHD dichotomized as a binary outcome. The candidate factors for subgroup identification included 10 baseline patient and donor characteristics, 18 immune subsets, and 7 plasma markers at day 28 after alloBMT for OS and aGVHD. All the variables are widely used in the field and have been established to correlate with alloBMT outcomes.[29-38] Day 28 was chosen because earlier predictive tools may allow for the development of impactful adaptive interventions. The splitting criteria in our tree models were maximum depth of 2 levels with at least 30 observations in a node necessary for a split and at least 15 observations in any terminal node for predicting OS and aGVHD after day 28. For the GVHD prediction model, we excluded patients who experienced grade 2 to 4 aGVHD within 28 days after alloBMT as patients already developed the queried outcome and to limit possible overlap with engraftment syndrome. All engrafting patients were included for OS analyses, and a conditional inference tree by binary recursive partitioning[39] was applied for detecting and classifying risk groups. The stopping rule for the OS tree model was measured by Bonferroni-adjusted P values $<.05$ for the partial null hypothesis of a single input marker.

For random forest predicting models,[40,41] 1000 trees were built, and the parameters for the optimal number of variables to try for splitting at each tree node and node size were tuned using out-of-bag (OOB) errors. Estimated variable importance (VIMP)[42] of each predictor in the corresponding random forest model was based on the differences of prediction error between predictor when randomly permuted vs the observed values. We used the top-ranked predictors from our tree/random forest models to guide selection of subsequent RNA sequencing (RNA-Seq) transcriptional studies. Due to a limited number of events, our random forest models were evaluated via OOB estimators.

Detailed descriptions of the platforms, outcome definitions, and group comparisons, as well as correlative analysis methods (flow cytometry, serum biomarker, and RNA-Seq) are outlined in the Supplemental Material available on the *Blood* Web site. Murine alloBMT studies were pursued to validate select RNA-Seq findings with regard to GVHD and establish the platform for future preclinical investigations. Analyses were carried out with the statistical software R version 3.6.0 (R Foundation for Statistical Computing, Vienna, Austria). All reported P values were 2-sided with significance level $<.05$ for hypothesis generating.

Results

Comparable quantitative immune recovery with effector memory cells predominating following PTCy platforms

We compared lymphocyte subset recovery among patients who received MSD MUD, and haplo alloBMT with PTCy (description of the groups provided in Table 1). First, we focused on characterizing the dynamics of the global lymphocyte reconstitution (Figure 1). Since there were no significant differences in analyzed parameters between MSD and MUD alloBMT recipients, MSD and MUD were combined into a single group matched for all subsequent analyses. Mean absolute lymphocyte counts (ALCs) on day 56 were 872 cells/μL after matched alloBMT and 1058 cells/μL after haplo alloBMT. Median ALCs were in the intraquartile range for normal donors (1500-2262 cells/μL) by 1 year after both haplo (median 1580 cells/μL) and matched (median 1320 cells/μL) alloBMT (Figure 1A). $CD3^+$ T cells followed a similar recovery pattern and reached pre-BMT levels by 6 months to 1 year (Figure 1A). B cell counts exceeded pre-BMT levels and were comparable to normal donors by 6 months after haplo and HLA-matched alloBMT (Figure 1A). NK cells recovered to normal donor levels by day 56 in all cohorts. There were no significant differences for reconstitution in ALC, $CD3^+$ T cells, B cells, and NK cells across the 3 PTCy cohorts (Figure 1A). However, analysis of T cell subsets revealed substantial differences at day 28 for both $CD4^+$ and $CD8^+$ T cells between HLA-matched and haplo alloBMT (P values $< .001$). By 2 months after alloBMT, $CD4^+$ T cells were similar after HLA-matched and haplo alloBMT. However, by 1 year, $CD4^+$ T cells were significantly lower after HLA-matched when compared with haplo alloBMT (218 cells/μL and 358 cells/μL, $P < .05$), and remained lower than the median donor counts (632, both P values $< .0001$). After day 28, $CD8^+$ T cells were comparable between haplo and HLA-matched alloBMT, exceeded pre-BMT levels, and reached normal donor levels by 6 months.

Downloaded from http://ashpublications.net/blood/article-pdf/139/4/608/1864234/bloodbld2021013054.pdf by guest on 07 May 2024

Table 1. Comparison of patient characteristics

Variable	MSD/MUD; n = 75	Haplo; n = 70 (%)
Median patient age, years (range)	49 (22-64)	41 (2-64)
Age <18, n (%)	0 (0)	14 (20)
Pre-BMT disease status, n (%)		
CR	45 (60)	34 (49)
MRD	14 (19)	11 (16)
Active disease	16 (21)	25 (35)
HCT-CI, median (range)	2 (0-8)	1 (0-5)
0-3, n (%)	49 (66)	64 (91)
≥3, n (%)	16 (21)	6 (9)
Median donor age: years (range)	41 (17-67)	38 (11-69)
Female → Male, n (%)	20 (27)	24 (34)
Recipient CMV positive, n (%)	39 (53)	28 (40)
CMV mismatch, n (%)	34 (45)	23 (33)
Cell dose infused, n (range)		
TNC x 10^8/kg	3.8 (0.32-8.82)	4.8 (2.63-11.2)
$CD34^+$ cells × 10^6/kg	3.3 (1-9.87)	4.5 (1.77-11.24)
$CD3^+$ cells × 10^7/kg	4.2 (1.5-30.28)	4.78 (1.09-11.7)

CMV, cytomegalovirus; CR, complete remission; haplo-HLA, haploidentical donor; HCT-CI, Hematopoietic Cell Transplantation-Comorbidity Index; MRD, minimal residual disease; MSD-HLA, matched sibling donor; MUD-HLA, matched unrelated donor; TNC, total nucleated cells.

Within $CD4^+$ and $CD8^+$ T cell subsets, naïve and central memory (CM) T cells were significantly lower than normal donors and pre-BMT levels for all time points. CM $CD8^+$ T cells were significantly lower after haplo alloBMT for all time points examined ($P < .0001$), but naïve and CM $CD4^+$ subsets were similar after HLA-matched and haplo alloBMT (Figure 1B-C). Effector memory (EM) and effector memory expressing RA (TEMRA) $CD4^+$ and $CD8^+$ were significantly lower at day 28 after haplo compared with HLA-matched alloBMT, but were not significantly different between donor type after that time point and reached the lower interquartile range of normal donor levels by 2 months. Overall, the dynamics of global lymphocyte reconstitution were similar in all cohorts with EM being the predominant phenotype of recovering T cells consistent with previous reports in HLA-matched alloBMT with conventional prophylaxis[43] and HLA-matched alloBMT using PTCy.[17]

Total numbers of Tregs were not significantly different by donor type, while conventional T cells (Tconv) were significantly lower at day 28 and significantly higher at 1 year ($P < .001$ and $P < .05$, respectively) after haplo alloBMT compared with HLA-matched recipients (Figure 1A-C). Development of aGVHD after day 28 was associated with decreased B cell counts but did not significantly affect overall immune reconstitution of other subsets (supplemental Figure 1). As such, subsequent analyses with additional markers sought to illuminate the interplay of molecular and cellular factors in the development of aGVHD.

Machine-learning analysis demonstrates Tconv recovery and CXCL9 plasma levels predict aGVHD development

Machine-learning approaches were then applied to investigate the relationship between cellular immune subsets and proteomic markers with clinical outcomes. For the whole cohort, incidences of grade 2 to 4 and grade 3 to 4 aGVHD were 38% (55/145) and 11% (16/145), respectively. We first used CART analyses to determine which cellular immune subsets and proteomic markers were associated with aGVHD development. We found that at day 28, higher CXCL9 levels accompanied by elevated Tconv levels were present in 28% of recipients and strongly associated with aGVHD development, with 60% of those patients experiencing aGVHD after day 28 (Figure 2A). In contrast, 52% of patients had low CXCL9 levels in whom there was an 11% incidence of aGVHD. Finally, 20% of patients fell into an intermediate risk category, having elevated CXCL9 but low Tconv, which was associated with a 24% incidence of aGVHD. Tconv and CXCL9 levels selected by CART analysis were used to perform cumulative incidence curves and significantly correlated with both grade 2 to 4 aGVHD and grade 3 to 4 aGVHD ($P < .00001$ and $P = .0002$, respectively) (Figure 2B).

Next, we performed VIMP conducted via random forest analysis to allow the identification of additional pertinent factors (Figure 2C). Similar to the CART analysis for aGVHD, CXCL9 was the top-ranked variable, followed by Tconv. The additional top-ranked variables included ST2, memory B cells, $CD4^+$ T cells,

Downloaded from http://ashpublications.net/blood/article-pdf/139/4/608/1864234/bloodbld2021013054.pdf by guest on 07 May 2024

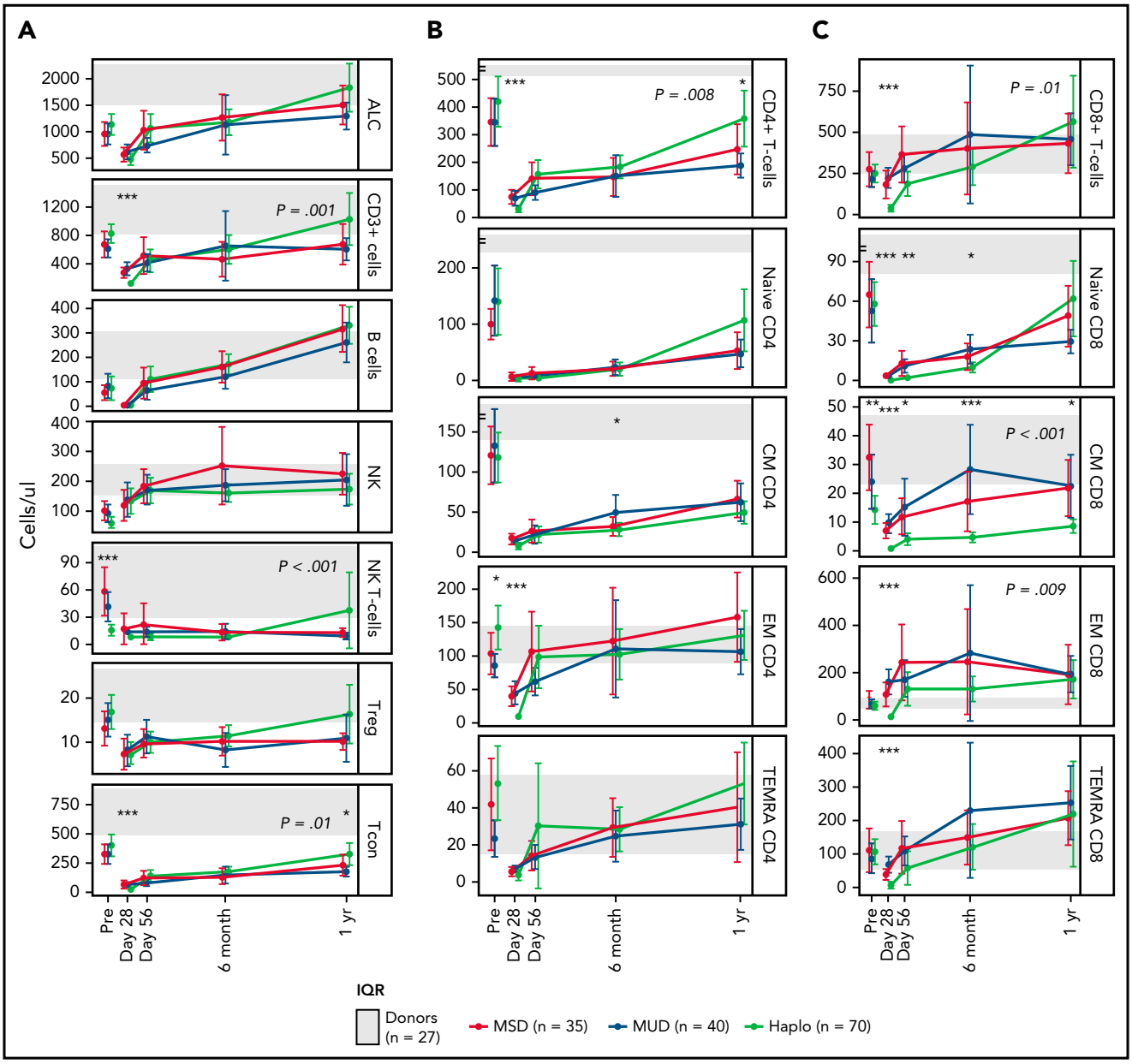

Figure 1. Similar immune reconstitution patterns after posttransplant cyclophosphamide platforms. Immune reconstitution patterns for individual cell subsets over time are shown. The red lines represent transplantation from HLA-MSD, blue lines represent transplantation from HLA-MUD, and green lines represent transplantation from HLA-haplo with the interquartile range of normal donors shown in the gray bar. The *P* values (*$P < .05$, **$P < .01$, ***$P < .001$) are for a global (familywise) ANOVA test of differences in the immune reconstitution patterns between 3 different platforms after BMT. Nonsignificant *P* values were not shown. *P* values for testing differences in immune reconstitution after alloBMT between MSD and MUD were all >.05. *P* values shown in the plots were for testing differences between immune reconstitution after haplo and combined MSD/MUD alloBMT, only *P* values < .05 are shown. There were no statistically significant differences between MSD and MUD after BMT with PTCy. When comparing haplo with MSD/MUD alloBMT, differences were observed in $CD3^+$ cells, Tconv, $CD4^+$ T cells, $CD8^+$ T cells, central memory (CM) $CD8^+$ and effector memory (EM), and effector memory expressing RA (TEMRA) $CD8^+$ cells. Differences in T cells were predominantly at day 28, where haplo alloBMT had lower absolute numbers, but these differences resolved over time for all subsets aside from CM $CD8^+$ T cells that remained lower after haplo alloBMT even at 1 year. There were no significant post-BMT differences between haplo and MSD/MUD alloBMT immune recovery for absolute lymphocyte counts (ALC), B cells, natural killer (NK) cells, regulatory T cells, naïve $CD4^+$ T cells, CM $CD4^+$ T cells, TEMRA $CD4^+$ T cells, or naïve $CD8^+$ T cells. Number of individual samples analyzed per time point is highlighted in supplemental Table 2.

BMT year, Reg3α, $CD38^+$ $CD4^+$ T cells, pre-BMT disease status, and age at BMT.

Transcriptional analyses suggest preserved Treg function in patients with aGVHD

Evaluation of Treg homeostasis in both haplo and HLA-matched cohorts suggests that the development of aGVHD was not associated with insufficient Treg numbers or impaired Treg/Tconv ratios (Figure 3A). To evaluate for molecular signatures of post-PTCy aGVHD, we pursued RNA-Seq of recovering lymphocyte subsets on peripheral blood mononuclear cells (PBMCs) collected on day 28 from the HLA-matched alloBMT recipients. To assess the longitudinal changes following post-PTCy aGVHD, available samples collected on day +180 were also sorted and sequenced.

Downloaded from http://ashpublications.net/blood/article-pdf/139/4/608/1864234/bloodbld2021013054.pdf by guest on 07 May 2024

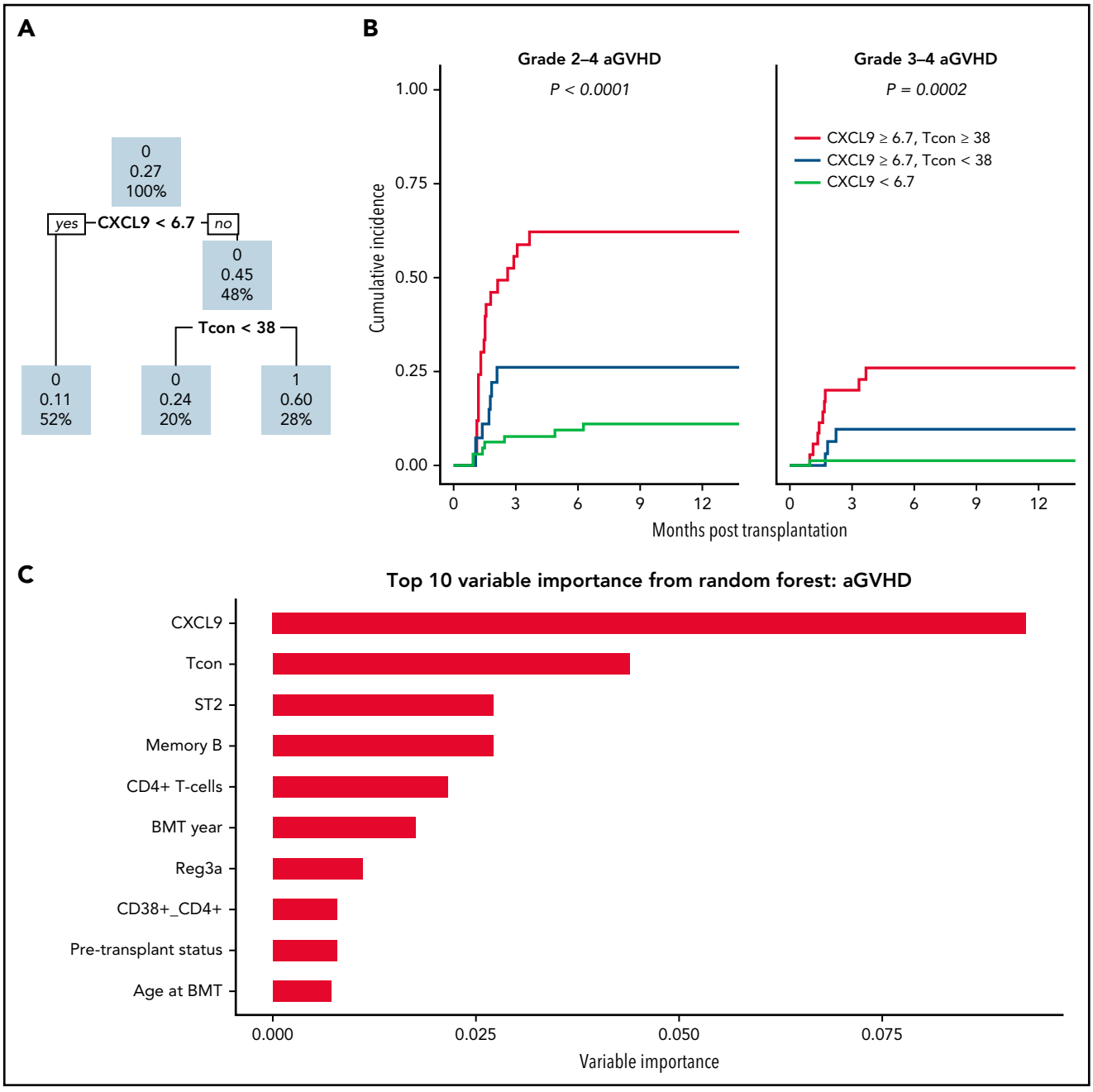

Figure 2. Machine-learning algorithms identify serum CXCL9 level and absolute T cell conventional cell numbers of aGVHD development following posttransplant cyclophosphamide-based myeloblative allogeneic BMT. (A) Using classification tree nodal selection at day 28 for prediction of aGVHD, the first tree branch was formed by CXCL9 levels <6.7, which made up 52% of recipients for whom the incidence of grade 2 to 4 aGVHD was 11%, which is less than the overall incidence after day 28 for the cohort of 28%. The second tree branch occurred within patients who had CXCL9 levels ≥6.7; those with conventional T cells (Tconv) <38 cells/μL represented 20% of patients and had an incidence of grade 2 to 4 aGVHD of 24%, whereas those with higher levels represented 28% of patients and had a 60% incidence of grade 2 to 4 aGVHD. The stopping rule was a minimum of 30 observations in a node and a minimum of 15 observations in the terminal node with a maximum of 2 depths of any node in the final tree. (B) Cumulative incidence curves based on the factors identified in the classification tree demonstrated that patients with high CXCL9 levels and high Tconv levels had the highest incidence of grade 2 to 4 and grade 3 to 4 aGVHD at 1 year (63% and 26%), whereas those with high CXCL9 levels and low Tconv counts at day 28 had intermediate rates of grade 2 to 4 and grade 3 to 4 aGVHD at 1 year (26% and 10%), and those with low CXCL9 levels had the lowest levels of grade 2 to 4 and grade 3 to 4 aGVHD at 1 year (11% and 1%). *P* values in Figure 2B were based on Gray's test without Bonferroni adjustment. Patients who experienced grade 2 to 4 or grade 3 to 4 aGVHD within 28 days after BMT were not included in this analysis due to the potential for overlap with engraftment syndrome and due to occurrence of GVHD before the biomarker collection at day 28. (C) Random forest regression analyses were then performed to identify the top 10 factors associated with aGVHD development. Similar to classification tree analyses, random forest identified CXCL9, followed by Tconv, as the variables most associated with aGVHD. ST2, memory B cells, $CD4^+$ T cells, BMT year, Reg3α, $CD38^+$ $CD4^+$ T cells, pre-BMT disease status, and age at BMT were also associated with aGVHD development.

Downloaded from http://ashpublications.net/blood/article-pdf/139/4/608/1864234/bloodbld2021013054.pdf by guest on 07 May 2024

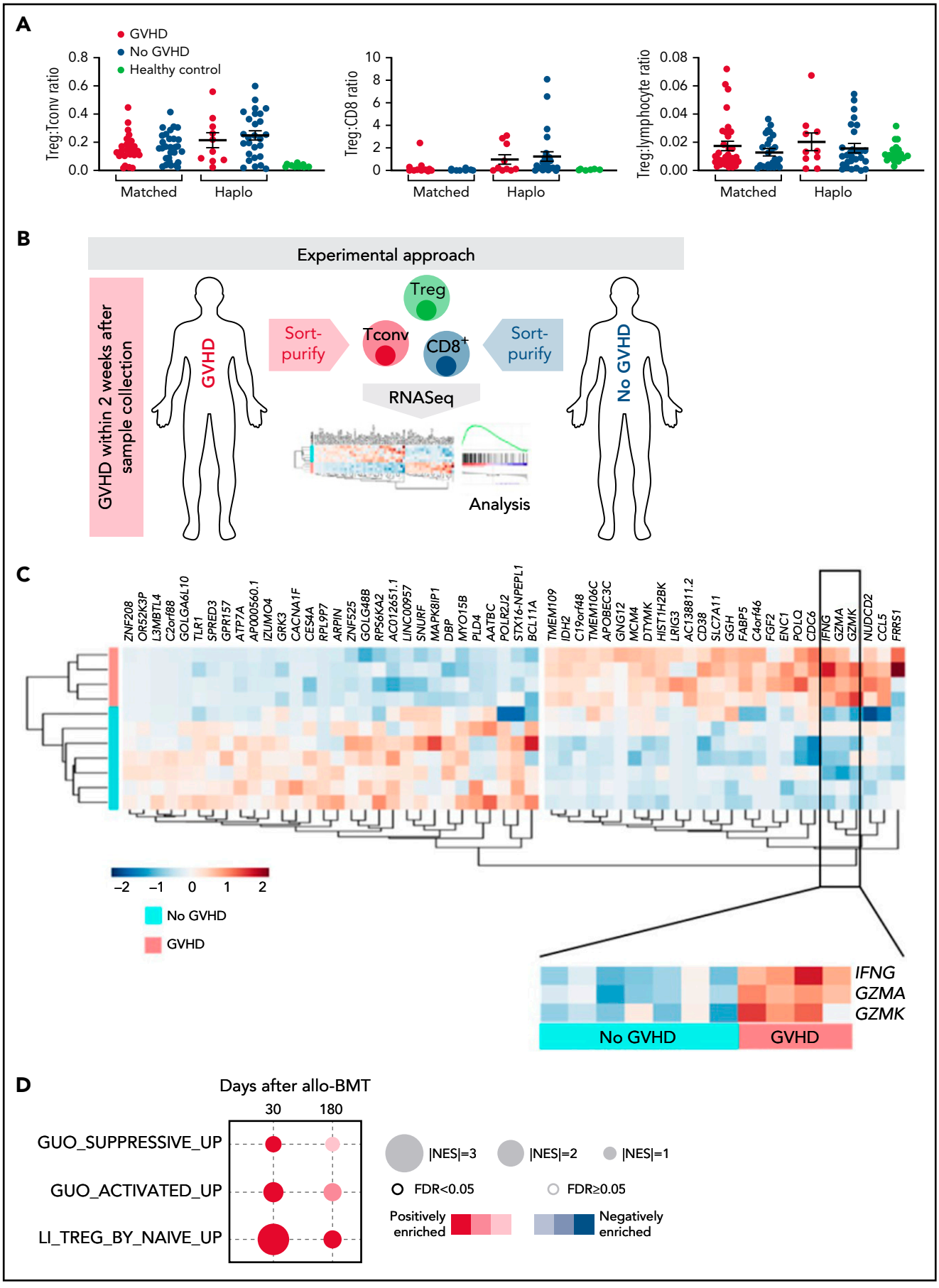

Figure 3. Preserved Treg cell numbers and function in patients developing aGVHD after posttransplant cyclophosphamide. aGVHD is characterized by preserved hallmarks of Treg functionality. (A) aGVHD after PTCy is not associated with loss of Treg/effector T cell balance. In both HLA-matched donor (MD) and haplo-BMT,

Downloaded from http://ashpublications.net/blood/article-pdf/139/4/608/1864234/bloodbld2021013054.pdf by guest on 07 May 2024

Differential gene expression analysis comparing Tregs from a subset of patients with or without aGVHD revealed 56 differentially expressed genes (DEGs) (30 downregulated) (Figure 3B; supplemental Table 3). In-depth analysis of the identified genes revealed that those necessary for bonafide Treg function and aGVHD protection, such as *IFNG* and *GZMA*,[44,45] were expressed at a significantly higher level in patients who developed aGVHD (Figure 3C). To define additional Treg transcriptional signatures and the relation of DEGs to aGVHD, we conducted gene set enrichment analysis (GSEA) using published gene sets. We found that the signatures of active and highly suppressive Treg profiles[46,47] were robustly enriched in Tregs from the cohort who developed aGVHD (NES 1.79, 2.16, and 3.38). Significant enrichment for these signatures was also present at later points after successful aGVHD treatment, but the difference was less pronounced (NES 1.50, 1.78, and 1.98) (Figure 3D).

Molecular profiling highlights effector Tconv impact on post-PTCy aGVHD

Next, we examined and compared the transcriptional profiles of $CD4^+$ Tconv and $CD8^+$ effector T cells from patients according to the development of aGVHD. Applying the same significance criteria as above, we identified a small number of DEGs in the $CD8^+$ T cells at day +28 (19 upregulated, 40 downregulated) (supplemental Figure 2; supplemental Table 4). However, we identified a total of 277 DEGs in the effector Tconv subset (Figure 4A; supplemental Table 5), of which 67 were upregulated in patients subsequently developing aGVHD. DEG analyses highlighted Th1-skewing and upregulation of interferon-regulated genes previously described as influencing GVHD development (*CXCR3*, *TBX21*).[48-50] Several inflammatory genes (*F2R*, *LGLS1*) were upregulated while those involved in apoptosis (*IER3*, *BCL2*) and the differentiation of pathogenic follicular helper cells (*C5AR1*)[51] were downregulated in GVHD cases. To evaluate long noncoding RNAs, which are influential in T cell immunity, we identified *Malat1*[52] and *Linc00402*[53] as downregulated in the aGVHD cohort (supplemental Figure 3).

The observation of CXCR3 upregulation reinforced our finding of increased serum levels of CXCL9, a CXCR3 ligand, as a predictor of aGVHD in our machine-learning analysis. To corroborate observed molecular changes linking Tconv and CXCL9 response, we performed flow cytometric analysis of patient PBMCs. Patients who developed grade 2 to 4 aGVHD showed significant enrichment for both CXCR3-expressing and Th17 ($CD146^+CCR5^+$)-prone Tconv when compared with patients without aGVHD and healthy donors ($P < .05$) (Figure 4B). Patients with GVHD also had a higher percentage of $CD146^+CCR5^+$ Tconv cells that coexpressed CXCR3. To extend the biological relevance of this finding, we evaluated changes in CXCR3 expression in a CD4-driven murine MHC-matched alloBMT model (B10.D2→BALB/c) (supplemental Methods). We confirmed CXCR3 upregulation during post-PTCy GVHD, observing increased numbers of $CXCR3^+$ Tconv in the spleens and livers of mice developing breakthrough GVHD (supplemental Figure 4).

We next compared observed molecular changes with datasets curated in MSigDB (Figure 4C). GSEA revealed that in the aGVHD cohort Kyoto Encyclopedia of Genes and Genomes (KEGG) GVHD signature enrichment was present in both Tconv and $CD8^+$ T cells, while Tconv were strongly enriched (NES >2) for the signatures of effector T cells (Figure 4C). We did not identify enrichment in the aGVHD cohort for pathways entertained as critical drivers of alloimmunity in aGVHD (Notch and IL6/JAK/STAT) (Figure 4C). Since the prior studies of PTCy activity in murine models suggested the creation of long-lasting T cell hyporesponsiveness[18] reminiscent of exhaustion, we indexed our data to landmark datasets that define exhaustion profiles occurring during the course of chronic infection and tumor-induced T cell dysfunction.[46,47,54-56] Lack of GVHD was not associated with an enrichment for gene expression signatures of exhausted $CD8^+$ T cells or Tconv (Figure 4F), suggesting that exhaustion is an unlikely mechanism behind PTCy protection against aGVHD. However, effector T cells sorted from patients who developed aGVHD exhibited the hallmarks of activation, including Th1/17 skewing in the Tconv compartment and a loss of a naïve $CD4^+$ Tconv signature. To evaluate if establishment and persistence of operational tolerance after PTCy may be related to delayed development of an exhaustion-like phenotype, we pursued RNA-Seq analyses of $CD8^+$ T cells and Tconv subsets from the aGVHD and the aGVHD-free cohort on day 180 after alloBMT. At that time, lack of enrichment for exhaustion in both $CD8^+$ T cells and Tconv persisted, but in contrast to earlier time points, there was enrichment for a naïve T cell signature (Figure 4E-F).

Metabolic hallmarks underscore Tconv selectivity in post-PTCy aGVHD

T cell activation during GVHD is a biologically robust process that requires extensive adaptation to augment cellular energy generation capabilities. Both glycolysis[57] and oxidative phosphorylation (OXPHOS)[58] are suggested as dominant processes in preclinical aGVHD models, and metabolic reprogramming is increasingly considered a putative therapeutic target in aGVHD.[59] We identified a robust enrichment for OXPHOS, fatty acid metabolism, and less so glycolysis in Tconv subset isolated from patients with aGVHD after HLA-matched alloBMT (Figure 5A). As selective enrichment was dominant in Tconv over the $CD8^+$ T cells subset (Figure 5A), we hypothesized that Tconv cells acquire unique functionality during post-PTCy aGVHD.

Figure 3 (continued) Treg ratios are preserved at day 28 after transplantation, irrespective of aGVHD development. (B-D) GVHD and GVHD-free matched donor alloBMT patient samples were collected on day 28 and day 180 and processed for RNA-Seq analysis of lymphocyte subsets, including $CD8^+$ T cells, conventional T cells (Tconv), and Treg. (B) Experimental workflow schema. (C) Tregs arising during post-PTCy aGVHD upregulate genes essential for Treg function. Hierarchical clustering analysis shows the top 60 differentially regulated genes between Tregs isolated from aGVHD (n = 4) and GVHD-free patients (n = 7) at day 28. *IFNG* and cytolytic effectors *GZMA/GZMK*, essential for Treg function, are highlighted in patients with aGVHD. (D) Enrichment analysis of Tregs on day 28 and day 180 from patients with aGVHD prior to aGVHD onset and after aGVHD control shows significant and positive enrichment for gene signatures identified as defining highly suppressive Tregs, with this phenotype persisting after aGVHD resolution.

Downloaded from http://ashpublications.net/blood/article-pdf/139/4/608/1864234/bloodbld2021013054.pdf by guest on 07 May 2024

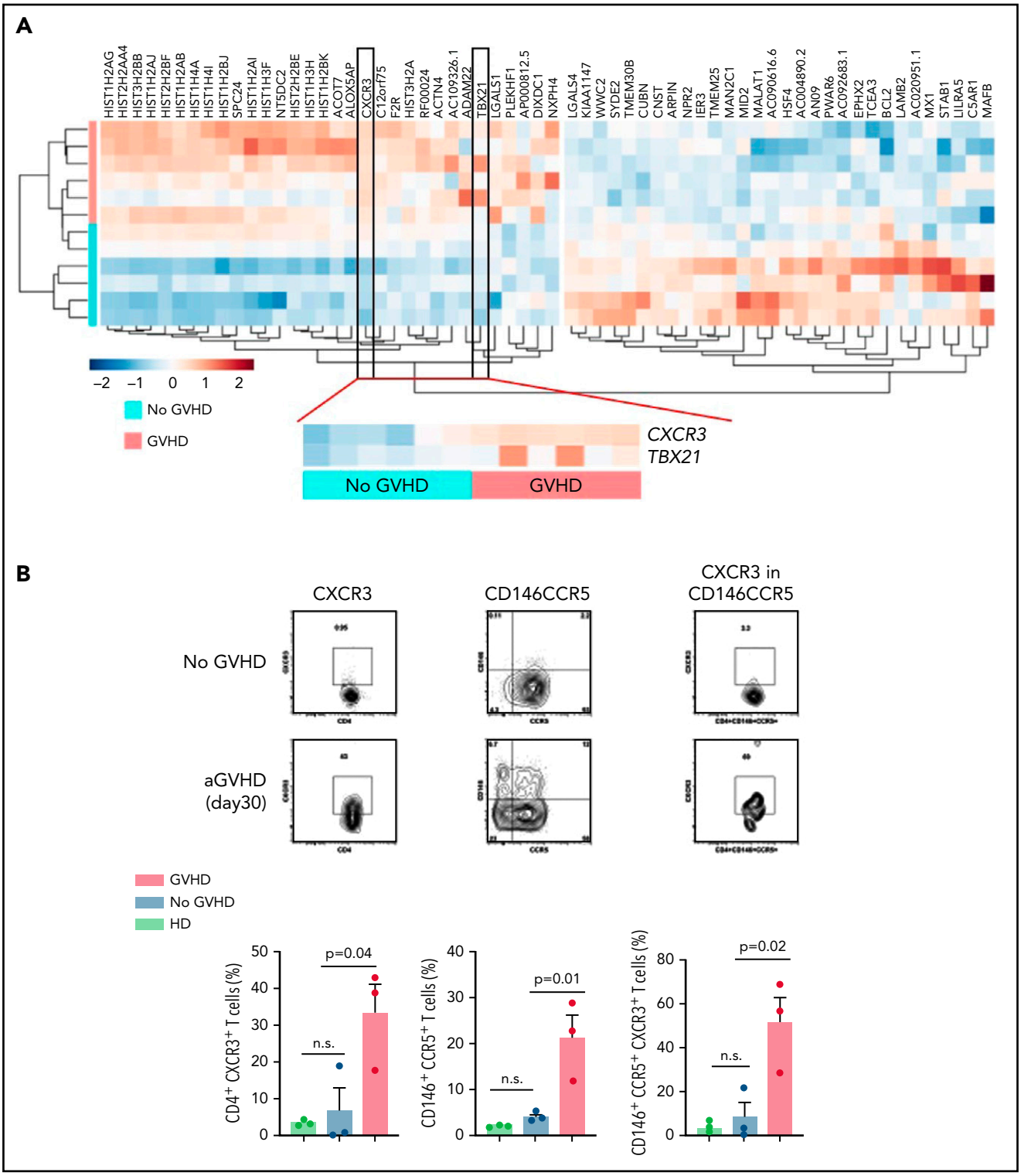

Figure 4. Upregulation of transcriptional activation markers in effector T cell subsets before aGVHD onset after posttransplant cyclophosphamide. Tconv but not CD8$^+$ T cell changes support selective role for CD4$^+$ T cells in aGVHD after PTCy. Analysis of DEGs in Tconv identifies proinflammatory skewing that proceeds aGVHD occurrence. (A) Hierarchical clustering of significantly regulated genes identified in Tconv RNA-Seq (aGVHD n = 6; GVHD-free n = 6) shows a greater differential regulation of gene expression with an enhancement of type 1 interferon response and Th1 skewing is the cohort of patients with aGVHD. (B) CXCR3, a key receptor for CXCL9, is upregulated on circulating allogeneic Tconv prior to the development of clinical post-PTCy breakthrough GVHD. Matched donor alloBMT patient samples were analyzed by flow cytometry for expression of CXCR3 on Tconv, including the Th17-prone CD146$^+$CCR5$^+$ subset. Representative flow cytometry panels are shown. (C) Gene set enrichment analyses validate Tconv and CD8$^+$ T cell activation during aGVHD, but not enhanced activity of Notch and IL-6/JAK/STAT pathways that have been associated in other studies with pathogenic alloresponse. Tconv (red) and CD8$^+$T cells (blue) analyses were performed using GSEA and Hallmark and c7 (immunologic signature) datasets from the MSigDb. (D) Transcriptional exhaustion is not associated with GVHD protection. Custom GSEA was performed using deposited datasets defining transcriptional hallmarks of functional T cell subsets. aGVHD development was associated with Tconv activation and loss of naïve signature. (E,F) Development of operational tolerance after PTCy is not associated with the acquisition of transcriptional exhaustion signature in CD8$^+$T cells or Tconv, but enhanced emergence of naïve effector T cell phenotypes. Comparative GSEA of day 180 CD8$^+$T cells (E) and Tconv (F) gene expression signatures from GVHD-free patients shows persistent lack of enrichment for exhaustion with progressive evolution of naïve phenotype, suggestive of evolving immune reconstitution.

Downloaded from http://ashpublications.net/blood/article-pdf/139/4/608/1864234/bloodbld2021013054.pdf by guest on 07 May 2024

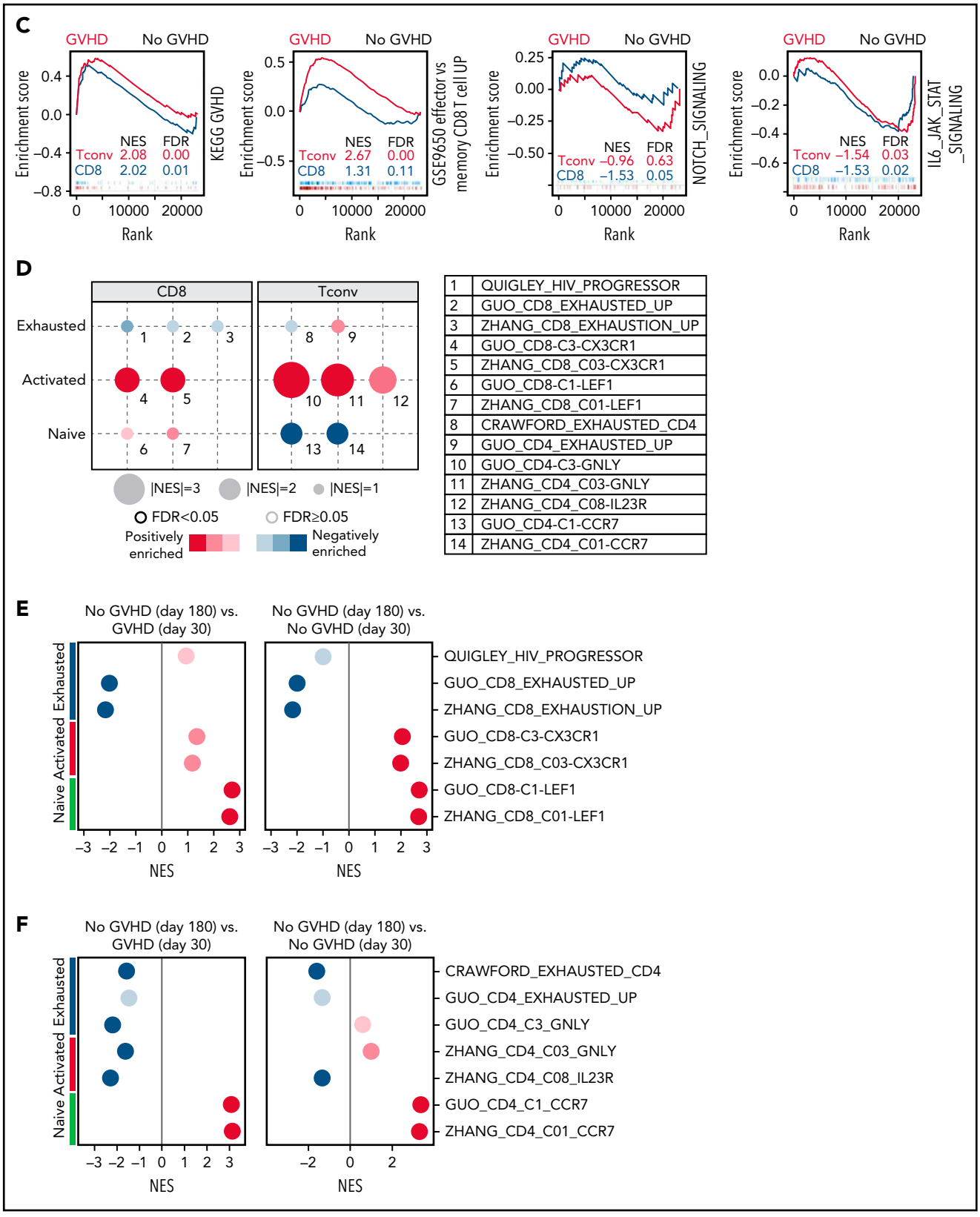

Figure 4. (Continued)

Downloaded from http://ashpublications.net/blood/article-pdf/139/4/608/1864234/bloodbld2021013054.pdf by guest on 07 May 2024

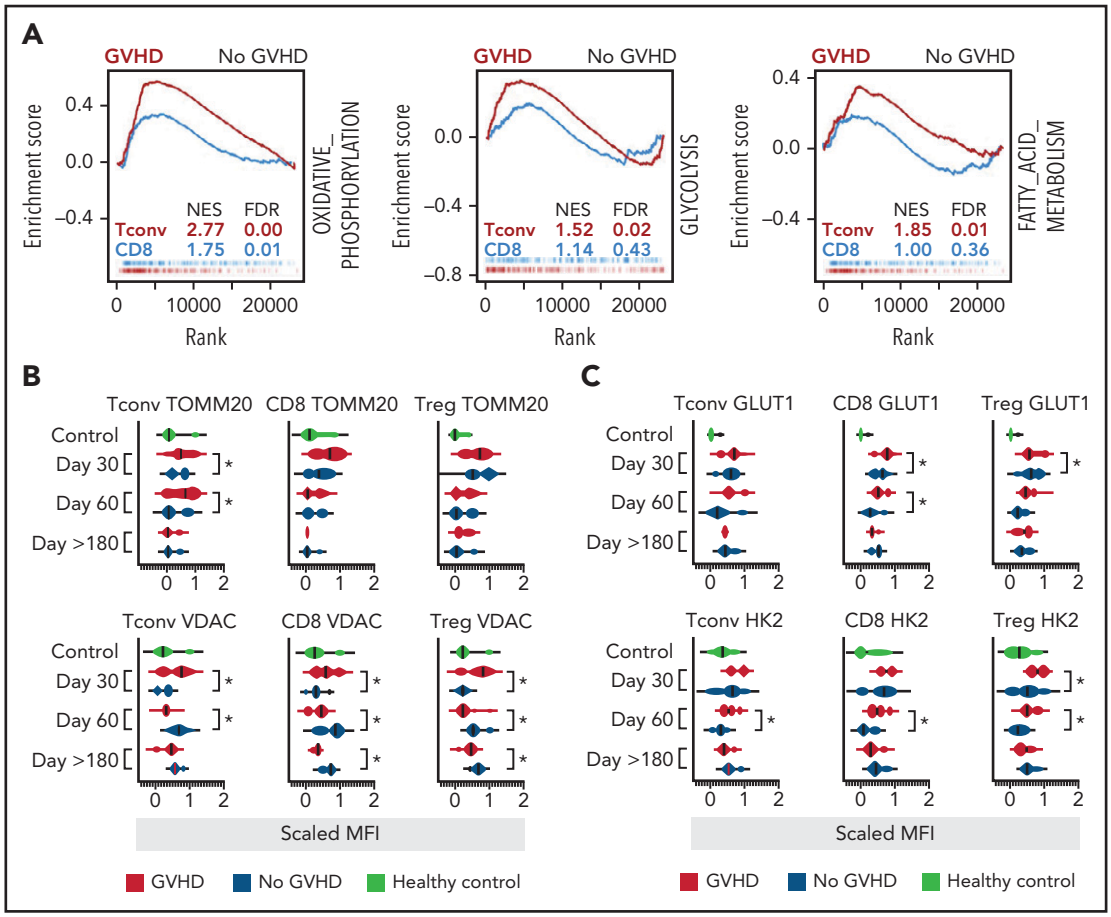

Figure 5. Enhanced metabolic signature in effector Tconv cells precedes breakthrough GVHD after posttransplant cyclophosphamide. Metabolic hallmarks of aGVHD after PTCy further the role for Tconv in the process. (A) GSEA using hallmark datasets from the MSigDb highlights dominantly enhanced metabolic signatures, including OXPHOS, Glycolysis, and fatty acid metabolism in Tconv (red) over CD8$^+$T cells (blue) in matched donor alloBMT patients developing aGVHD. (B-C) Hallmarks of augmented metabolic function in aGVHD are seen in Tconv recovered from aGVHD patients early before disease development (aGVHD n = 8; GVHD-free n = 7; healthy control n = 6). (B) Expression of TOMM20 (essential for import and assembly of respiratory chain complexes) and VDAC (mitochondrial porin essential for OXPHOS and glycolysis coupling), and (C) GLUT1, a key glucose transporter, and hexokinase 2, an enzyme catalyzing glucose phosphorylation, was quantified in patient samples at defined time points after alloBMT. Cumulative scaled MFI data for all time points and heatmap highlighting individual patient changes on day 28 is shown.

Accordingly, we pursued metabolic flow cytometric studies[60] to evaluate key glycolysis-related transporters (GLUT1 and HK2), mitochondrial transport proteins (TOMM20, necessary for import and assembly of respiratory chain complexes[61]), and mitochondrial porins (VDAC, linking glycolysis and OXPHOS[62]). Consistent with transcriptional studies, we observed an enhanced OXPHOS signature with TOMM20 and VDAC expression in Tconv (less so in CD8$^+$ T cells and Treg subsets) in the aGVHD cohort and an overall augmented metabolic profile when compared with patients without GVHD and donor controls (Figure 5B). These same patients demonstrated a trend to enhanced glycolysis on day 28, although with heterogenous effects across the lymphocyte subsets (Figure 5C).

Machine-learning analyses for survival identify the importance of NK cell recovery

Having probed the predictors of aGVHD after PTCy use, we next focused on detecting those that impact OS and identified NK cell recovery as the main determinant. To give context, median numbers of NK cells in HLA-matched and haplo alloBMT cohorts at day 28 were similar at 54 cells/μL and 66 cells/μL, respectively. Using CART, NK cell count ≤50.5 cells/μL at day 28 emerged as the only significant risk marker for OS (Figure 6A). Two-year OS and progression-free survival (PFS) for recipients with NK cells >50.5 cells/μL were 81% (95% CI: 72% to 90%) and 76% (95% CI: 67% to 86%) compared with 50% (95% CI: 39% to 64%) and 44% (95% CI: 34% to 59%) for those with NK cells ≤50.5 cells/μL ($P < .00001$ and $P \leq .0001$, respectively) (Figure 6B). We then performed cumulative incidence curves by NK cell counts >50.5 cells/μL (Figure 6B) and found that both relapse (21% compared with 35% at 2 years, $P = .04$) and NRM (4% compared with 21%, $P = .004$) were significantly lower in those with higher NK cell counts. Next, we performed VIMP via random forest analysis to identify additional predictors of OS (Figure 6C). NK cell count was again the top selected factor. Other selected factors in order of the strength of association included pre-BMT disease status, ST2, Naïve CD4$^+$ T cells, TNFR1, graft CD3$^+$ cell dose, CXCL9, Reg3α, alloBMT year, and plasmablast counts.

Cellular and molecular signatures of relapse identify disrupted NK cell homeostasis

We next sought to evaluate the phenotype and functional hallmarks of reconstituting NKs after PTCy-based alloBMT. Initial

Downloaded from http://ashpublications.net/blood/article-pdf/139/4/608/1864234/bloodbld2021013054.pdf by guest on 07 May 2024

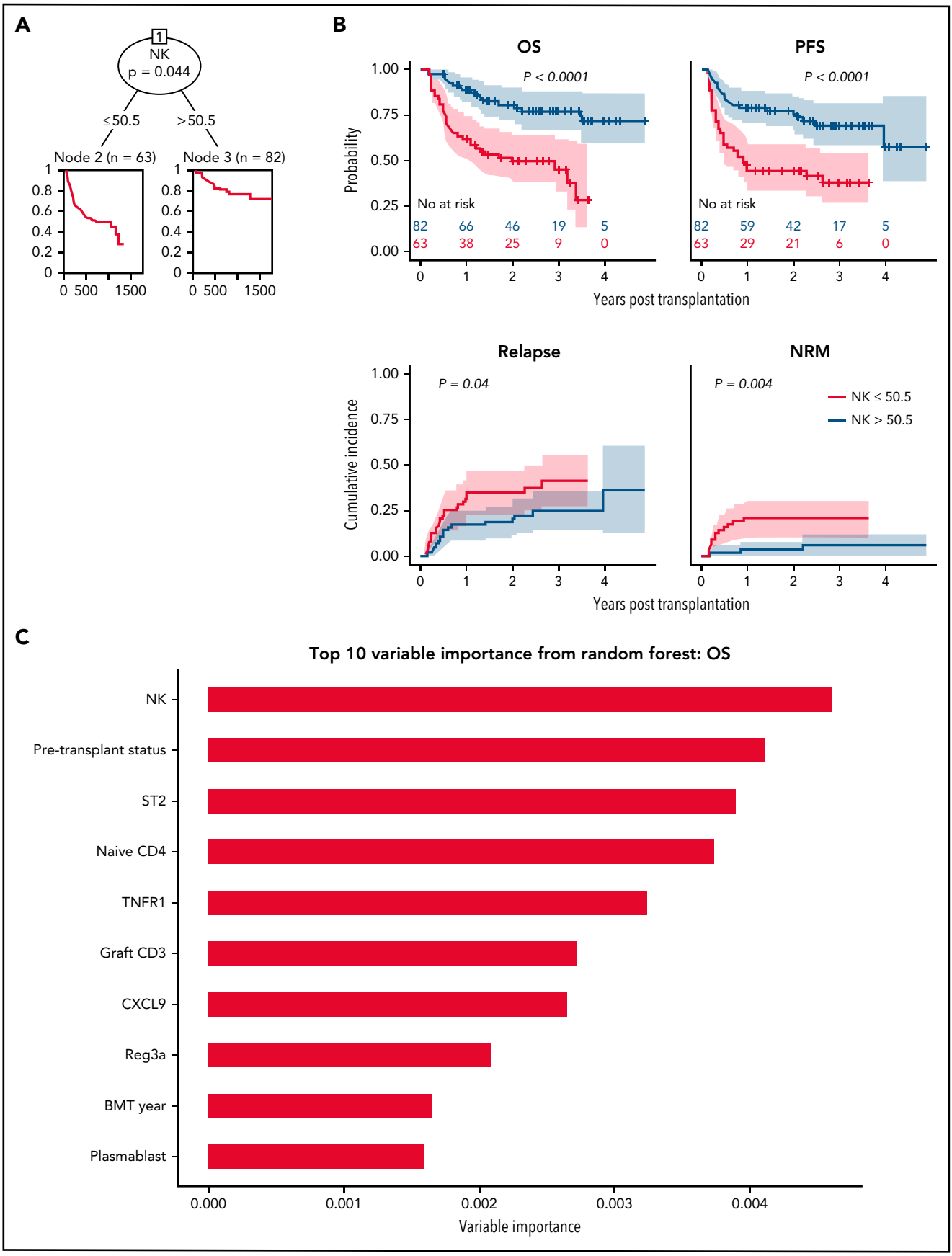

Figure 6. Less NK cell recovery after posttransplant cyclophosphamide-based allogeneic BMT predicts inferior survival. (A) Classification tree nodal selection at day 28 for OS showed that the only branch was formed by NK cells counts >50.5 cells/μL, which occurred in 82 patients (blue curves), counts were lower in 63 patients

Downloaded from http://ashpublications.net/blood/article-pdf/139/4/608/1864234/bloodbld2021013054.pdf by guest on 07 May 2024

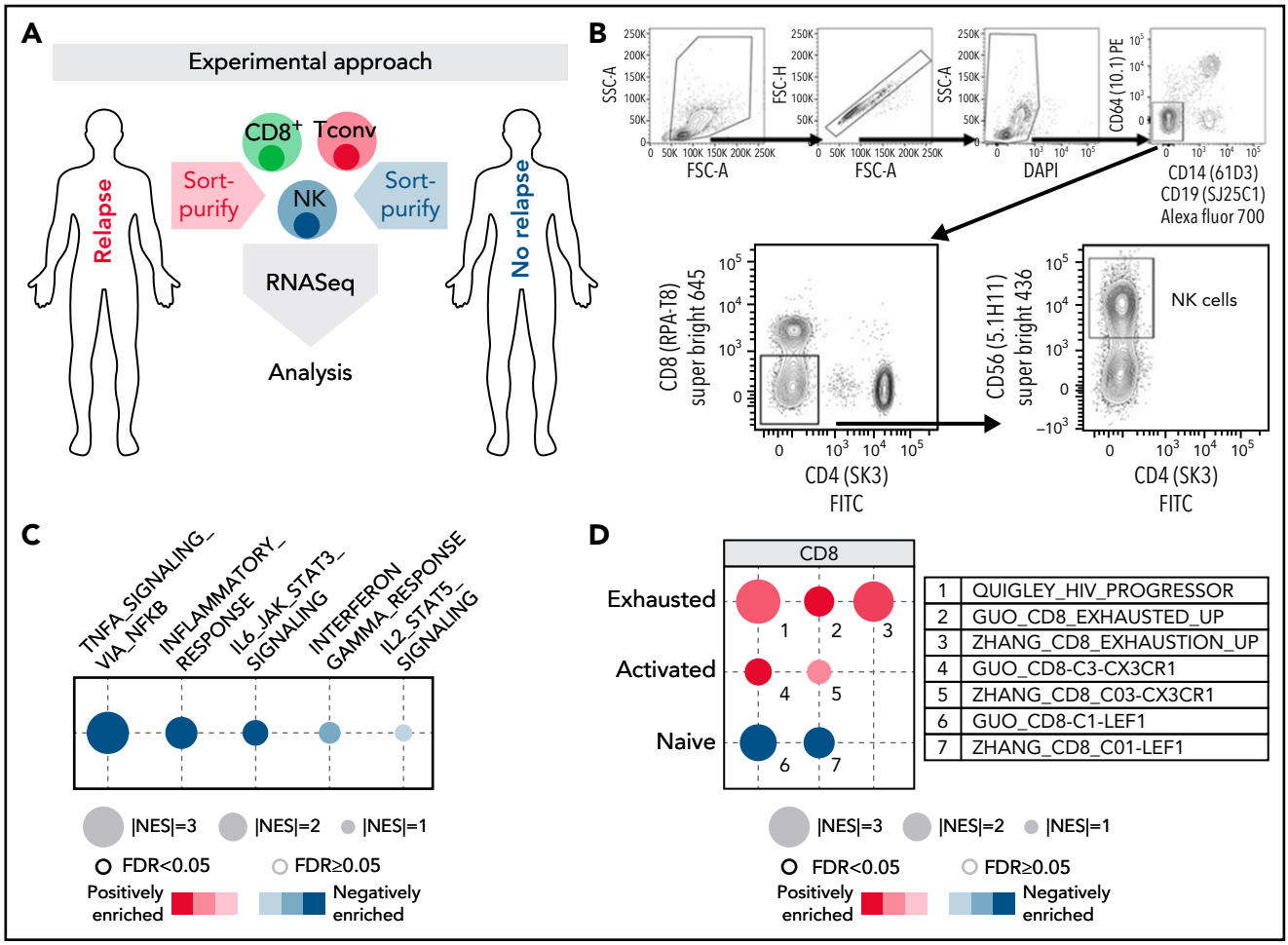

Figure 7. Dampened NK inflammatory signaling and CD8$^+$ T cell exhaustion precedes early relapse after posttransplant cyclophosphamide allogeneic BMT. The transcriptional landscape of NK cells CD8$^+$ T cells in haploidentical alloBMT suggests development of effector function paralysis in relapse. Experimental workflow schema (A) and flow cytometry sort strategy (B) are shown. (C) Gene set enrichment analyses identified loss of inflammatory signatures in NK cells isolated from haplo alloBMT recipients who relapsed, with a dominant effect on TNF-α signaling. Analyses were performed using GSEA and hallmark dataset from the MSigDb (relapse n = 5; relapse-free n = 8). (D) Emergence of transcriptional exhaustion in haplo alloBMT CD8$^+$ T cells also proceeded primary disease relapse. Custom GSEAs were performed using deposited datasets defining transcriptional hallmarks of functional T cell subsets. Subsequent development of disease relapse was positively associated with the acquisition of exhaustion and progressive loss of naïve CD8$^+$ T cell phenotypes, suggesting impaired immune reconstitution (relapse n = 5; relapse-free n = 5).

characterization of the recovering NK cells in haplo and HLA-matched alloBMT recipients confirmed that the most immature population of NK cells (CD56^{bright}CD16^{neg}) predominated at day 28 in all cohorts (supplemental Figure 5A), which was consistent with our previous findings and those of Rambaldi et al in different haplo cohorts using PTCy.[20,21] CD56^{bright}CD16^{int} NK cells comprised a higher percentage of the NK cells at all time points after alloBMT when compared with healthy donors. Recovery of CD56^{dim}CD16^{pos} NK cells in both donor cohorts was slow and only reached the normal distribution at year 1 post-BMT (supplemental Figure 5B). The percentage of CD56^{neg}CD16^{pos} was similar to that of normal donors throughout all time points.

Prior studies have shown that loss of NK functionality (decreased production of TNF-α and IFN-γ) early after alloBMT predicts enhanced relapse.[63] To test if a similar phenotype occurred with post-PTCy relapse, we focused on the haplo alloBMT cohort and sort-purified NK cells from PBMCs obtained on day 28 after alloBMT (Figure 7A,B). Relapse was associated with profound alterations in multiple inflammatory signaling pathways, with key impacts on TNF-α signaling (Figure 7C). NK cells retrieved from relapsing patients exhibited transcriptional aberrancies, distinguishing them from those identified in naïve and functional NK cells[64] (Supplemental Figure 6). In addition, we profiled CD8$^+$ T cells isolated from the same patients and identified enrichment for a molecular signature of exhaustion, with the loss of naïve

Figure 6 (continued) (red curves). The stopping rule included *P* value < .05 after Bonferroni testing, a minimum of 30 observations in a node, and a minimum of 15 observations in the terminal node. The *P* value in the figure is after Bonferroni correction. (B) The top curves show OS and PFS Kaplan Meier curves by the NK cell levels selected by the classification tree (>50.5 cells/μL vs ≤50.5 cells/μL). The bottom curves show the cumulative incidence curves for relapse and nonrelapse mortality (NRM) by NK cell levels selected by the classification. The blue curves represent recipients in whom NK cell counts at day 28 were >50.5 cells/μL, and the red curves represent the recipients with NK cell counts at day 28 ≤50.5 cells/μL.

Downloaded from http://ashpublications.net/blood/article-pdf/139/4/608/1864234/bloodbld2021013054.pdf by guest on 07 May 2024

CD8$^+$ T cell hallmarks (Figure 7). Taken together, these data suggest that disease recurrence may be heralded by both the numerical disadvantage of NK cell reconstitution and transcriptional hallmarks of NK dysfunction and CD8$^+$ T cell exhaustion.

Discussion

As the first study to directly compare immune reconstitution after PTCy-based MSD, MUD, and haplo alloBMT, we provide critical insights into the patterns of immune recovery and the landscape of PTCy-induced tolerance. First, we found comparable quantitative reconstitution of NK and B cells after all platforms, but a transient early delay in CD4$^+$ and CD8$^+$ T cell recovery in the haplo alloBMT cohort that may be attributable to their additional immunosuppression and abrogated by discontinuation of MMF at day 35. Rapid EM and TEMRA CD4$^+$ and CD8$^+$ T cell recovery supports the low rates of PTLD and infectious deaths after PTCy.[13,65]

Our work also highlights a distinct landscape of tolerance that arises with PTCy use. Enrichment of bonafide effector Treg signatures and preserved Treg numbers argue against the loss of Treg-driven tolerance as the key mechanism of post-PTCy breakthrough aGVHD. We hypothesize that the expansion and functionality of Tregs during an aGVHD event after PTCy may be compensatory, contribute to steroid responsiveness, and prevent the development of severe aGVHD or cGVHD, although this requires testing in future studies. Tconv enrichment for activation pathways, accompanied by lack of such enrichment in CD8$^+$ T cells, adds to the growing evidence of the key role of CD4$^+$ T cells in alloimmunity.[66,67] Further, we identify Tconv recovery, when coupled with elevated CXCL9, a CXCR3 ligand, and type 1 interferon-regulated chemokine that promotes leukocyte tissue egress, as a critical feature in aGVHD development after PTCy. Transcriptional and proteomic upregulation of CXCR3 on Tconv in both patients and mice further underscores the importance of this partnership in post-PTCy aGVHD. Whether the CXCL9-CXCR3-Tconv axis can be exploited as a prognostic or predictive biomarker or as a therapeutic target remains to be tested in future studies.

While PTCy-driven aGVHD protection was attributed to CD8$^+$ T cell hyporesponsiveness in murine models,[18] our data suggest that the role for CD8$^+$ T cells may be more limited in post-PTCy aGVHD. In our cohort, the classical hallmarks of T cell exhaustion were not associated with protection from GVHD, but may be relevant to the risk of disease recurrence, a finding that requires further testing. Since PTCy has been associated with improved survival and less aGVHD in patients exposed to immune checkpoint blockade pre-BMT,[68,69] our data may support the use of checkpoint blockade after PTCy-based alloBMT to augment graft-versus-leukemia responses without an augmented risk of aGVHD.

Our immunophenotypic studies also yield insight into relapse risk after PTCy allografting, uncovering decreased early NK counts as a key predictor of reduced OS due to increases in both relapse and NRM. These data are augmented by evidence of impaired inflammatory functioning in NK cells and exhausted CD8$^+$ T cells in patients who ultimately relapsed. The observed global dysfunction included a multitude of cytokine-signaling driven pathways and acquisition of dysfunctional NK phenotype. We also demonstrated that gene expression in NK cells on day 28 in patients who did not relapse was consistent with the functional capacity reported by Pical-Izard et al.[63] These observations lend further credence to the pursuit of relapse prevention with the transfer of expanded mature NK cells[70] and provide directions for future biomarker-driven adaptive therapy instituted early after BMT. Shortcomings of our study include the relatively small numbers of patients available for bulk immune subset sequencing, emphasizing the need for future transcriptome analyses in aGVHD, including single-cell sequencing of effector T cells in target tissues. Furthermore, future studies should also seek to independently validate our machine-learning findings.

In summary, we identify the limited impact of HLA-matching on the robust and rapid immune reconstitution patterns following PTCy-based myeloablative conditioning alloBMT. Slight differences in the timing of T cell recovery are best explained by the use of additional immunosuppression and younger median recipient age in the haplo cohort. While our data does not allow for a direct comparison with allografting using conventional GVHD prophylaxis, a recent study lends further credence to our emphasis on CD4$^+$ T cell dysregulation during post-PTCy GVHD.[71] We also provide molecular insights into the putative operational mechanisms of PTCy by coupling transcriptional observations with the results of machine-learning studies to identify Tconv as key mediators of aGVHD and NK numbers and functional signatures as critical to underlying disease control. Our work highlights the unique immune landscape after PTCy and hints at GVHD mechanisms distinct from those reported with calcineurin-based allografting. Whether the same paradigms apply to the nonmyeloablative or PBMC-based allografting strategies, where G-CSF mobilization-related imprinting creates distinct immune circuitry, remains to be explored. Given that immune reconstitution is a dynamic process, selective use of day 28 studies to feed the machine-learning algorithms may be another limitation. However, this served well our goal of identifying early posttransplant changes that may be exploited for development of adaptive strategies to prevent or treat GVHD and to optimize graft-versus-tumor effects. For instance, targeting the CXCR3-CXCL9 axis may prove beneficial in aGVHD control or prevention. In addition, harnessing NK cells to minimize relapse will be explored in our ensuing work.

Acknowledgments

The authors thank Edus H. Warren, Borje S. Andersson, and Paul V. O'Donnell for contribution to the original NCT00809276 studies and Sofia Berglund for NK phenotypic analysis.

This work was supported by grants from the NIH/NHLBI (R01HL110907) and Otsuka Pharmaceutical to L.L., V.R. (K08HL145116), J.D.P. (R01HL110907), and NIH/NCI to S.P. (R01CA168814) and to L.L., R.J.J., and K.R.C. (NIH/NCI P01CA225618, P30CA006973). Career Development Award from the American Society for Transplantation and Cellular Therapy (V.R.) and Huntsman Cancer Foundation (V.R.). Work presented in this publication was made possible through the use of the NIH/NCI P01CA225618 Immune Monitoring Core (L.L.); JH-TIE Shared resource (NIH/NIBIB P41EB028239); University of Utah and the Huntsman Cancer Institute Shared Resource Services (NIH/NCI P30CA042014; NIH/NCI 1S10RR026802-01).

Authorship

Contribution: S.R.M., V.R., and L.L. were involved in the study's conception and design, data collection, analysis, laboratory analyses and interpretation, primary writing of the manuscript, and manuscript revisions; H.L.T.

Downloaded from http://ashpublications.net/blood/article-pdf/139/4/608/1864234/bloodbld2021013054.pdf by guest on 07 May 2024

and R.V. statistically analyzed and interpreted the data and revised the manuscript; C.G.K., A.V., S.I., E.T., B.L., and D.A. were involved in data collection and laboratory analyses; and C.G.K., S.P., K.R.C., R.J.J., J.D.P., and H.J.S. were also involved in analysis, conception and design, and revised the manuscript; and all authors approved the manuscript.

Conflict-of-interest disclosure: S.R.M. Grant/research/clinical trial support: Gilead Sciences, Aprea Therapeutics, McCabe Fund. V.R. Grant/research/clinical trial support: Syndax Pharmaceuticals. Consultant/advisory board: Regeneron Pharmaceuticals. S.P. Patent holder on "Biomarkers and assays to detect chronic graft versus host disease" (U.S. patent 10 571,478 B2). L.L. Patent holder: WindMiL Therapeutics. Grant/research/clinical trial support: Genentech. Consultant/advisory boards: Gilead Sciences, Rubius Therapeutics, PrecisionBiosciences, Talaris Therapeutics. The remaining authors declare no competing financial interests.

ORCID profiles: V.R., 0000-0002-9699-1157; S.P., 0000-0001-5571-2775.

Correspondence: Leo Luznik, Johns Hopkins University, The Bunting-Blaustein Cancer Research Building, 1650 Orleans St Room 2M08, Baltimore, MD 21287; e-mail: luznile@jhmi.edu; and Vedran Radojcic, University of Utah Huntsman Cancer Institute, 2000 Circle of Hope Dr, Rm 5263, Salt Lake City, UT 84112; e-mail: vedran.radojcic@hsc.utah.edu.

Footnotes

Submitted 24 June 2021; accepted 24 September 2021; prepublished online on *Blood* First Edition 17 October 2021. DOI 10.1182/blood.2021013054.

*S.R.M. and V.R. contributed equally to this study.

†V.R. and L.L. are joint senior authors.

Presented in part at the Transplantation and Cellular Therapy Meetings 2020.

The online version of this article contains a data supplement.

There is a *Blood* Commentary on this article in this issue.

The publication costs of this article were defrayed in part by page charge payment. Therefore, and solely to indicate this fact, this article is hereby marked "advertisement" in accordance with 18 USC section 1734.

Downloaded from http://ashpublications.net/blood/article-pdf/139/4/608/1864234/bloodbld2021013054.pdf by guest on 07 May 2024

REFERENCES

1. Savani BN, Mielke S, Rezvani K, et al. Absolute lymphocyte count on day 30 is a surrogate for robust hematopoietic recovery and strongly predicts outcome after T cell-depleted allogeneic stem cell transplantation. *Biol Blood Marrow Transplant.* 2007;13(10):1216-1223.

2. Le Blanc K, Barrett AJ, Schaffer M, et al. Lymphocyte recovery is a major determinant of outcome after matched unrelated myeloablative transplantation for myelogenous malignancies. *Biol Blood Marrow Transplant.* 2009;15(9):1108-1115.

3. Ishaqi MK, Afzal S, Dupuis A, Doyle J, Gassas A. Early lymphocyte recovery post-allogeneic hematopoietic stem cell transplantation is associated with significant graft-versus-leukemia effect without increase in graft-versus-host disease in pediatric acute lymphoblastic leukemia. *Bone Marrow Transplant.* 2007;41(3):245-252.

4. Aversa F, Tabilio A, Velardi A, et al. Treatment of high-risk acute leukemia with T-cell-depleted stem cells from related donors with one fully mismatched HLA haplotype. *N Engl J Med.* 1998;339(17):1186-1193.

5. Roux E, Dumont-Girard F, Starobinski M, et al. Recovery of immune reactivity after T-cell-depleted bone marrow transplantation depends on thymic activity. *Blood.* 2000;96(6):2299-2303.

6. Handgretinger R, Lang P, Schumm M, et al. Immunological aspects of haploidentical stem cell transplantation in children. *Ann N Y Acad Sci.* 2006;938(1):340-357, discussion 357-358.

7. Komanduri KV, St John LS, de Lima M, et al. Delayed immune reconstitution after cord blood transplantation is characterized by impaired thymopoiesis and late memory T-cell skewing. *Blood.* 2007;110(13):4543-4551.

8. Kanakry CG, Tsai HL, Bolaños-Meade J, et al. Single-agent GVHD prophylaxis with posttransplantation cyclophosphamide after myeloablative, HLA-matched BMT for AML, ALL, and MDS. *Blood.* 2014;124(25):3817-3827.

9. McCurdy SR, Kanakry JA, Showel MM, et al. Risk-stratified outcomes of nonmyeloablative HLA-haploidentical BMT with high-dose posttransplantation cyclophosphamide. *Blood.* 2015;125(19):3024-3031.

10. McCurdy SR, Kanakry CG, Tsai HL, et al. Development of grade II acute graft-versus-host disease is associated with improved survival after myeloablative HLA-matched bone marrow transplantation using single-agent posttransplant cyclophosphamide. *Biol Blood Marrow Transplant.* 2019;25(6):641-650.

11. Luznik L, O'Donnell PV, Symons HJ, et al. HLA-haploidentical bone marrow transplantation for hematologic malignancies using nonmyeloablative conditioning and high-dose, posttransplantation cyclophosphamide. *Biol Blood Marrow Transplant.* 2008;14(6):641-650.

12. Brunstein CG, Fuchs EJ, Carter SL, et al; Blood and Marrow Transplant Clinical Trials Network. Alternative donor transplantation after reduced intensity conditioning: results of parallel phase 2 trials using partially HLA-mismatched related bone marrow or unrelated double umbilical cord blood grafts. *Blood.* 2011;118(2):282-288.

13. Kanakry JA, Kasamon YL, Bolaños-Meade J, et al. Absence of posttransplantation lymphoproliferative disorder after allogeneic blood or marrow transplantation using posttransplantation cyclophosphamide as graft-versus-host disease prophylaxis. *Biol Blood Marrow Transplant.* 2013;19(10):1514-1517.

14. Solh MM, Baron J, Zhang X, et al. Differences in graft-versus-host disease characteristics between haploidentical transplantation using posttransplantation cyclophosphamide and matched unrelated donor transplantation using calcineurin inhibitors. *Biol Blood Marrow Transplant.* 2020;26(11):2082-2088.

15. Kanakry CG, Ganguly S, Zahurak M, et al. Aldehyde dehydrogenase expression drives human regulatory T cell resistance to posttransplantation cyclophosphamide. *Sci Transl Med.* 2013;5(211):211ra157.

16. Ganguly S, Ross DB, Panoskaltsis-Mortari A, et al. Donor $CD4^+$ $Foxp3^+$ regulatory T cells are necessary for posttransplantation cyclophosphamide-mediated protection against GVHD in mice. *Blood.* 2014;124(13):2131-2141.

17. Kanakry CG, Coffey DG, Towlerton AM, et al. Origin and evolution of the T cell repertoire after posttransplantation cyclophosphamide. *JCI Insight.* 2016;1(5):e86252.

18. Wachsmuth LP, Patterson MT, Eckhaus MA, Venzon DJ, Gress RE, Kanakry CG. Post-transplantation cyclophosphamide prevents graft-versus-host disease by inducing alloreactive T cell dysfunction and suppression. *J Clin Invest.* 2019;129(6):2357-2373.

19. Ross D, Jones M, Komanduri K, Levy RB. Antigen and lymphopenia-driven donor T cells are differentially diminished by posttransplantation administration of cyclophosphamide after hematopoietic cell transplantation. *Biol Blood Marrow Transplant.* 2013;19(10):1430-1438.

20. Russo A, Oliveira G, Berglund S, et al. NK cell recovery after haploidentical HSCT with posttransplant cyclophosphamide: dynamics and clinical implications. *Blood.* 2018;131(2):247-262.

21. Rambaldi B, Kim HT, Reynolds C, et al. Impaired T- and NK-cell reconstitution after haploidentical HCT with posttransplant cyclophosphamide. *Blood Adv.* 2021;5(2):352-364.

22. Kanakry CG, Bakoyannis G, Perkins SM, et al. Plasma-derived proteomic biomarkers in human leukocyte antigen-haploidentical

or human leukocyte antigen-matched bone marrow transplantation using posttransplantation cyclophosphamide. *Haematologica*. 2017;102(5):932-940.

23. Van Nieuwenhove E, Lagou V, Van Eyck L, et al. Machine learning identifies an immunological pattern associated with multiple juvenile idiopathic arthritis subtypes. *Ann Rheum Dis*. 2019;78(5): 617-628.

24. Robinson GA, Peng J, Dönnes P, et al. Disease-associated and patient-specific immune cell signatures in juvenile-onset systemic lupus erythematosus: patient stratification using a machine-learning approach. *Lancet Rheumatol*. 2020;2(8):e485-e496.

25. Robinson G, Peng J, Donnes P, et al. OP0287 a machine learning approach for precision stratification of Juvenile-Onset Sle. *Ann Rheum Dis*. 2020;79(suppl 1):1799.

26. Kanakry CG, O'Donnell PV, Furlong T, et al. Multi-institutional study of posttransplantation cyclophosphamide as single-agent graft-versus-host disease prophylaxis after allogeneic bone marrow transplantation using myeloablative busulfan and fludarabine conditioning. *J Clin Oncol*. 2014; 32(31):3497-3505.

27. Symons HJ, Zahurak M, Cao Y, et al. Myeloablative haploidentical BMT with posttransplant cyclophosphamide for hematologic malignancies in children and adults. *Blood Adv*. 2020;4(16):3913-3925.

28. Breiman L, Friedman JH. Tree-structured classification via generalized discriminant analysis: comment. *J Am Stat Assoc*. 1988; 83(403):725-727.

29. Storek J, Dawson MA, Storer B, et al. Immune reconstitution after allogeneic marrow transplantation compared with blood stem cell transplantation. *Blood*. 2001;97(11):3380-3389.

30. Maecker HT, McCoy JP, Nussenblatt R. Standardizing immunophenotyping for the Human Immunology Project. *Nat Rev Immunol*. 2012;12(3):191-200.

31. Adom D, Rowan C, Adeniyan T, Yang J, Paczesny S. Biomarkers for allogeneic HCT outcomes. *Front Immunol*. 2020;11:673.

32. DeZern AE, Franklin C, Tsai H-L, et al. Relationship of donor age and relationship to outcomes of haploidentical transplantation with posttransplant cyclophosphamide. *Blood Adv*. 2021;5(5): 1360-1368.

33. Kollman C, Howe CWS, Anasetti C, et al. Donor characteristics as risk factors in recipients after transplantation of bone marrow from unrelated donors: the effect of donor age. *Blood*. 2001;98(7):2043-2051.

34. Ljungman P, Brand R, Hoek J, et al; Infectious Diseases Working Party of the European Group for Blood and Marrow Transplantation. Donor cytomegalovirus status influences the outcome of allogeneic stem cell transplant: a study by the European group for blood and marrow transplantation. *Clin Infect Dis*. 2014; 59(4):473-481.

35. Schmidt-Hieber M, Tridello G, Ljungman P, et al. The prognostic impact of the cytomegalovirus serostatus in patients with chronic hematological malignancies after allogeneic hematopoietic stem cell transplantation: a report from the Infectious Diseases Working Party of EBMT. *Ann Hematol*. 2019;98(7):1755-1763.

36. Sorror ML, Logan BR, Zhu X, et al. Prospective validation of the predictive power of the hematopoietic cell transplantation comorbidity index: a center for international blood and marrow transplant research study. *Biol Blood Marrow Transplant*. 2015;21(8):1479-1487.

37. Loren AW, Bunin GR, Boudreau C, et al. Impact of donor and recipient sex and parity on outcomes of HLA-identical sibling allogeneic hematopoietic stem cell transplantation. *Biol Blood Marrow Transplant*. 2006;12(7): 758-769.

38. McCurdy SR, Kanakry CG, Tsai H-L, et al. Grade II acute graft-versus-host disease and higher nucleated cell graft dose improve progression-free survival after HLA-haploidentical transplant with posttransplant cyclophosphamide. *Biol Blood Marrow Transplant*. 2018;24(2):343-352.

39. Hothorn T, Hornik K, Zeileis A. Unbiased recursive partitioning: a conditional inference framework. *J Comput Graph Stat*. 2006;15(3):651-674.

40. Breiman L. Random forests. *Mach Learn*. 2001;45(1):5-32.

41. Ishwaran H, Kogalur UB, Blackstone EH, Lauer MS. Random survival forests. *Ann Appl Stat*. 2008;2(3):841-860.

42. Ishwaran H. Variable importance in binary regression trees and forests. *Electron J Stat*. 2007;1(none):519-537.

43. Latis E, Michonneau D, Leloup C, et al; CRYOSTEM Consortium. Cellular and molecular profiling of T-cell subsets at the onset of human acute GVHD. *Blood Adv*. 2020;4(16):3927-3942.

44. Koenecke C, Lee CW, Thamm K, et al. IFN-γ production by allogeneic Foxp3+ regulatory T cells is essential for preventing experimental graft-versus-host disease. *J Immunol*. 2012;189(6):2890-2896.

45. Velaga S, Ukena SN, Dringenberg U, et al. Granzyme A is required for regulatory T-cell mediated prevention of gastrointestinal graft-versus-host disease. *PloS One*. 2015; 10(4):e0124927.

46. Guo X, Zhang Y, Zheng L, et al. Global characterization of T cells in non-small-cell lung cancer by single-cell sequencing. *Nat Med*. 2018;24(7):978-985.

47. Li H, van der Leun AM, Yofe I, et al. Dysfunctional CD8 T cells form a proliferative, dynamically regulated compartment within human melanoma. *Cell*. 2019;176(4):775-789.e18.

48. Duffner U, Lu B, Hildebrandt GC, et al. Role of CXCR3-induced donor T-cell migration in acute GVHD. *Exp Hematol*. 2003;31(10):897-902.

49. Piper KP, Horlock C, Curnow SJ, et al. CXCL10-CXCR3 interactions play an important role in the pathogenesis of acute graft-versus-host disease in the skin following allogeneic stem-cell transplantation. *Blood*. 2007;110(12):3827-3832.

50. Fu J, Wang D, Yu Y, et al. T-bet is critical for the development of acute graft-versus-host disease through controlling T cell differentiation and function. *J Immunol*. 2014;194(1):388-397.

51. Verghese DA, Chun N, Paz K, et al. C5aR1 regulates T follicular helper differentiation and chronic graft-versus-host disease bronchiolitis obliterans. *JCI Insight*. 2018; 3(24):124646.

52. Hewitson JP, West KA, James KR, et al. *Malat1* suppresses immunity to infection through promoting expression of Maf and IL-10 in Th cells. *J Immunol*. 2020;204(11): 2949-2960.

53. Peltier D, Radosevich M, Hou G, et al. RNA-seq of human T-cells after hematopoietic stem cell transplantation identifies Linc00402 as a novel regulator of T-cell alloimmunity. *bioRxiv*. 2020: 2020.2004.2016.045567.

54. Quigley M, Pereyra F, Nilsson B, et al. Transcriptional analysis of HIV-specific $CD8^+$ T cells shows that PD-1 inhibits T cell function by upregulating BATF. *Nat Med*. 2010;16(10):1147-1151.

55. Crawford A, Angelosanto JM, Kao C, et al. Molecular and transcriptional basis of $CD4^+$ T cell dysfunction during chronic infection. *Immunity*. 2014;40(2):289-302.

56. Zhang L, Yu X, Zheng L, et al. Lineage tracking reveals dynamic relationships of T cells in colorectal cancer. *Nature*. 2018; 564(7735):268-272.

57. Nguyen HD, Chatterjee S, Haarberg KM, et al. Metabolic reprogramming of alloantigen-activated T cells after hematopoietic cell transplantation. *J Clin Invest*. 2016;126(4):1337-1352.

58. Byersdorfer CA, Tkachev V, Opipari AW, et al. Effector T cells require fatty acid metabolism during murine graft-versus-host disease. *Blood*. 2013;122(18): 3230-3237.

59. Tijaro-Ovalle NM, Karantanos T, Wang H-T, Boussiotis VA. Metabolic targets for improvement of allogeneic hematopoietic stem cell transplantation and graft-vs.-host disease. *Front Immunol*. 2019;10:295.

60. Thompson EA, Cascino K, Ordonez AA, et al. Metabolic programs define dysfunctional immune responses in severe COVID-19 patients. *Cell Rep*. 2021;34(11):108863.

61. Formosa LE, Ryan MT. Mitochondrial OXPHOS complex assembly lines. *Nat Cell Biol*. 2018;20(5):511-513.

62. Maldonado EN. VDAC-tubulin, an anti-Warburg pro-oxidant switch. *Front Oncol*. 2017;7:4.

63. Pical-Izard C, Crocchiolo R, Granjeaud S, et al. Reconstitution of natural killer cells in HLA-matched HSCT after reduced-intensity

Downloaded from http://ashpublications.net/blood/article-pdf/139/4/608/1864234/bloodbld2021013054.pdf by guest on 07 May 2024

conditioning: impact on clinical outcome. *Biol Blood Marrow Transplant.* 2015;21(3): 429-439.

64. Yang C, Siebert JR, Burns R, et al. Heterogeneity of human bone marrow and blood natural killer cells defined by single-cell transcriptome. *Nat Commun.* 2019;10(1):3931.

65. Crocchiolo R, Bramanti S, Vai A, et al. Infections after T-replete haploidentical transplantation and high-dose cyclophosphamide as graft-versus-host disease prophylaxis. *Transpl Infect Dis.* 2015;17(2):242-249.

66. Yeh A, Jagasia M, Dahlman K, et al. Cytomegalovirus promotes aberrant memory CD4 T cell differentiation and immune function after allogeneic stem cell transplantation. *Blood.* 2020; 136(Suppl 1):15-16.

67. Watkins B, Qayed M, McCracken C, et al. Phase II trial of Costimulation blockade with abatacept for prevention of acute GVHD. *J Clin Oncol.* 2021;39(17): 1865-1877.

68. Schoch LK, Cooke KR, Wagner-Johnston ND, et al. Immune checkpoint inhibitors as a bridge to allogeneic transplantation with posttransplant cyclophosphamide. *Blood Adv.* 2018;2(17):2226-2229.

69. Oran B, Garcia-Manero G, Saliba RM, et al. Posttransplantation cyclophosphamide improves transplantation outcomes in patients with AML/MDS who are treated with checkpoint inhibitors. *Cancer.* 2020; 126(10):2193-2205.

70. Ciurea SO, Kongtim P, Soebbing D, et al. Decrease posttransplant relapse using donor-derived expanded NK-cells. *Leukemia.* 2021. https://doi.org/10.1038/s41375-021-01349-4

71. Khimani F, Ranspach P, Elmariah H, et al. Increased infections and delayed CD4+ T-cell but faster B-cell immune reconstitution after posttransplant cyclophosphamide compared to conventional GVHD prophylaxis in allogeneic transplantation. *Transplant Cell Ther.* 2021; 27(11):940-948.

Downloaded from http://ashpublications.net/blood/article-pdf/139/4/608/1864234/bloodbld2021013054.pdf by guest on 07 May 2024